Journal of Magnetic Resonance 193 (2008) 233–242

Contents lists available at ScienceDirect

Journal of Magnetic Resonance

journal homepage: www.elsevier.com/locate/jmr

^{29}Si NMR in solid state with CPMG acquisition under MAS

J.W. Wiench [a], V.S.-Y. Lin [b], M. Pruski [b,*]

[a] U.S. DOE Ames Laboratory, Iowa State University, Ames, IA 50011, USA
[b] Department of Chemistry and U.S. DOE Ames Laboratory, Iowa State University, Ames, IA 50011, USA

ARTICLE INFO

Article history:
Received 22 February 2008
Revised 8 May 2008
Available online 20 May 2008

Keywords:
Solid-state NMR
^{29}Si NMR
CPMG acquisition
J-coupling
MAS
HETCOR

ABSTRACT

A remarkable enhancement of sensitivity can be often achieved in ^{29}Si solid-state NMR by applying the well-known Carr–Purcell–Meiboom–Gill (CPMG) train of rotor-synchronized π pulses during the detection of silicon magnetization. Here, several one- and two-dimensional (1D and 2D) techniques are used to demonstrate the capabilities of this approach. Examples include 1D ^{29}Si{X} CPMAS spectra and 2D ^{29}Si{X} HETCOR spectra of mesoporous silicas, zeolites and minerals, where X = ^{1}H or ^{27}Al. Data processing methods, experimental strategies and sensitivity limits are discussed and illustrated by experiments. The mechanisms of transverse dephasing of ^{29}Si nuclei in solids are analyzed. Fast magic angle spinning, at rates between 25 and 40 kHz, is instrumental in achieving the highest sensitivity gain in some of these experiments. In the case of ^{29}Si–^{29}Si double-quantum techniques, CPMG detection can be exploited to measure homonuclear *J*-couplings.

1. Introduction

Silicon-29 is one of the most widely studied nuclei in solid-state NMR spectroscopy. Numerous reviews have detailed the applications of ^{29}Si NMR to the study of silicates [1], silica surfaces [2], silicon alloys [3], ceramics [4], glasses [5], and other crystalline and amorphous materials [6,7]. The vast majority of these studies have relied on one-dimensional (1D) experiments performed using direct ^{29}Si polarization (DP) or ^{29}Si{^{1}H} cross polarization (CP), magic angle spinning (MAS) and ^{1}H decoupling using a radiofrequency (RF) magnetic field. Two-dimensional (2D) methods have also been employed, e.g., in CP-based ^{29}Si{^{1}H} heteronuclear (HETCOR) NMR studies of organic/inorganic nanocomposites [8–11], zeolites [12], silica [13], and mesoporous aluminosilicates [14]. Two-dimensional methods for obtaining ^{29}Si–^{29}Si correlation spectra that exploit double-quantum (DQ) through-bond (scalar) or through-space (dipolar) interactions have been reported, as well [15–17].

However, wider exploitation of multi-dimensional solid-state NMR methods is hindered by low ^{29}Si sensitivity, which results from low natural abundance of spin-1/2 isotope (4.7%), small gyromagnetic ratio, and unusually slow longitudinal relaxation. Fortunately, the presence of a long relaxation time T_1 in inorganic solids is often accompanied by a long transverse dephasing (decoherence) time T_2^{CPMG}, defined here as the decay time of the echo train due to time-dependent interactions that are non-refocusable by the Carr–Purcell–Meiboom–Gill [18] (CPMG) sequence of π pulses combined with MAS and/or RF decoupling schemes. This makes it possible to detect the signal multiple times at intervals that are longer than the free induction decay (FID) observed following the single-pulse excitation (often denoted as T_2^*) but much shorter than T_1.

The multiple pulse CPMG sequence, which refocuses inhomogeneous line broadening and reduces homonuclear dipolar broadening in solids, was first introduced to measure the decay of transverse nuclear magnetization [19,20]. It later found applications in various areas of magnetic resonance spectroscopy, including experiments with field gradients or strongly inhomogeneous static fields (e.g., imaging [21–23] and diffusion measurements [24–26]), high-resolution liquid-state NMR (solvent peak suppression [27,28], HETCOR experiments [29–31], and exchange studies [32]), homonuclear distance measurements in solids [33,34] and electron spin resonance (ESR) [35,36].

In solid-state NMR applications, the most appealing advantage offered by the CPMG pulse sequence is the sensitivity gain resulting from refocusing the magnetization multiple times. Indeed, enhancement of the signal-to-noise (S/N) ratio has been demonstrated in various studies where low natural abundance, a low gyromagnetic ratio (γ), long relaxation time T_1, large line width or any combination of these factors rendered 'standard' averaging of FIDs impractical. These studies used static [37–42], MAS [40,41,43], MQMAS [44,45], and PHORMAT [46] experiments with spin-1/2 and quadrupolar nuclei.

In spite of long decoherence times of silicon nuclei, the CPMG technique has been used only rarely in ^{29}Si NMR. The strategy was applied in a study of silicates (α-crystobalite and Zircon), where the sensitivity of ^{29}Si MAS spectra was increased by an order of magnitude using a rotor-synchronized CPMG sequence [47] and

* Corresponding author. Fax: +1 515 294 0266.
E-mail address: mpruski@iastate.edu (M. Pruski).

1090-7807/$ - see front matter © 2008 Elsevier Inc. All rights reserved.
doi:10.1016/j.jmr.2008.05.007

at least fivefold signal enhancement was reported in 2D ^{29}Si{^{1}H} heteronuclear correlation (HETCOR) experiments on clay minerals, where the ^{29}Si signal was stretched by means of multiple echoes at the expense of the chemical shift information [48].

We recently demonstrated that highly resolved ^{29}Si{^{1}H} HETCOR NMR spectra of silica-based catalytic systems can be obtained with excellent sensitivity using multiple pulse CPMG refocusing and appropriate data processing [49,50]. These experiments were made possible by the use of fast MAS, at rates of 25–40 kHz, which provided adequate ^{1}H–^{1}H decoupling. More importantly, fast MAS allowed the heteronuclear decoupling to be performed using low RF power, which was essential in these experiments due to unusually long acquisition periods (up to several seconds).

Herein, we analyze the utility of CPMG refocusing in a number ^{29}Si NMR techniques, and discuss the experimental strategies that maximize sensitivity, as well as the future applications of these methods. Examples of 1D ^{29}Si{X} CPMAS spectra, 2D ^{29}Si{X} HETCOR (X = ^{1}H and ^{27}Al) spectra and ^{29}Si–^{29}Si DQMAS homonuclear correlation spectra are shown. This effort was largely motivated by our interest in studying the mesoporous catalytic materials, which is reflected in the choice of samples for this study.

2. Experimental

2.1. NMR resonance

Most of the experiments were performed at 14.1 T on a Varian NMR System 600 spectrometer, equipped with 3.2 and 1.6 mm triple-resonance MAS probes, which can accommodate 22 and 8 μL of sample and reach rotation frequencies of 25 and 45 kHz, respectively. The ^{29}Si{^{27}Al} and DQ ^{29}Si–^{29}Si{^{1}H} spectra were acquired at 9.4 T on a Chemagnetics Infinity spectrometer using 5 mm triple-resonance probe operated at the MAS rates of 8–10 kHz. The pulse sequence used in 2D ^{29}Si{X} experiments (Fig. 1a) is similar to that used in our earlier study [49]. The same sequence was used in 1D CPMAS experiments by setting $t_1 = 0$. The DQMAS homonuclear correlation experiments (Fig. 1b) utilized the ^{29}Si{^{1}H} CP followed by the INADEQUATE scheme for excitation and reconversion of DQ coherences [51–53]. The π pulses were always applied synchronously with the rotor.

The experimental parameters are given in figure captions using the following symbols: B_0 denotes the magnetic field strength, ν_R the sample rotation rate, ν_{RF}^X the magnitude of the RF magnetic field applied to the X spins, τ_{CP} the cross polarization time, N_{CPMG} the number of echoes acquired in CPMG experiments, τ_{CPMG} the corresponding time interval between π pulses, τ_{RD} the relaxation delay, and NS the number of scans. The chemical shifts of ^{1}H, ^{29}Si, and ^{27}Al are reported using the δ scale and are referenced to tetramethylsilane (TMS) and 1 M aluminum(III) nitrate ($Al(NO_3)_3$) solution at 0 ppm.

2.2. Samples

Most of the CPMG-based experiments are conducted using three samples of MCM-41-type mesoporous silica nanoparticle (MSN) materials whose synthesis and characterization have been described in our earlier reports: (i) a non-functionalized sample, referred to as MSN [54]; (ii) a sample functionalized via co-condensation with covalently bound allyl groups (—CH_2—CH=CH_2), referred to as AL–MSN [54]; and (iii) a sample functionalized via grafting with chloromethyltriethoxysilane (($EtO)_3Si(CH_2Cl)$), referred to as CMTES–MSN [50]. Based on the deconvolution of ^{29}Si DPMAS spectra, we estimated that 11 ± 2% and 15 ± 2% of all silicon atoms in AL–MSN and CMTES–MSN, respectively, are bound to carbon (functionalized) [50,54]. All silicas were studied in the absence of templating molecules, which were removed by acid extraction (MSN and AL–MSN) or calcination (CMTES–MSN). The measurements were typically performed with samples packed in MAS rotors after exposure to ambient conditions in the laboratory. In the case of AL–MSN the spectra were obtained after the inorganic hydrogen atoms on the surface had been eliminated by exchange with deuterium. For these measurements the material was packed using a glove bag.

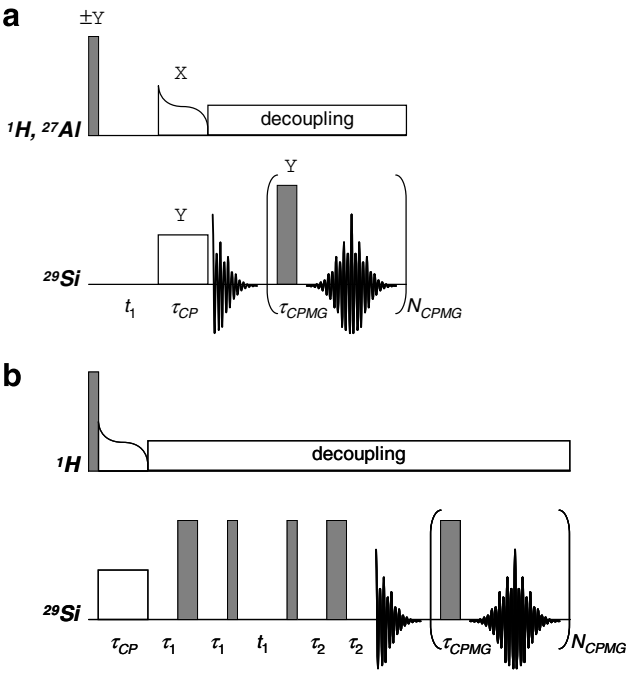

Fig. 1. Pulse sequences for 2D ^{29}Si NMR experiments with CPMG detection: (a) ^{29}Si{^{1}H} and ^{29}Si{^{27}Al} HETCOR, (b) ^{29}Si–^{29}Si{^{1}H} refocused INADEQUATE. Solid rectangles represent π and $\pi/2$ pulses, whereas open pulses represent cross polarization and decoupling. In sequence (a), the phases are the same as in reference [49], with the receiver phase being inverted in concert with the phase of $\pi/2$ pulse in the ^{1}H channel. In sequence (b), the phase cycling during INADEQUATE is the same as in reference [53]. The phases of π pulses used in the CPMG sequence followed the phase of the last (refocusing) pulse in INADEQUATE. In addition, the hypercomplex method was used to achieve quadrature detection in the v_1 dimension in all 2D experiments.

To demonstrate the ^{29}Si{^{27}Al} methods, two commercially available samples were used. Andesine (sodium calcium aluminum silicate, $Na_{0.7-0.5}Ca_{0.3-0.5}Al_{1.3-1.5}Si_{2.7-2.5}O_8$) is a naturally occurring mineral belonging to the plagioclase series of the feldspar family. Plagioclase is a solid solution series, also known as the plagioclase feldspar series, which ranges from albite ($NaAlSi_3O_8$) to anorthite ($CaAl_2Si_2O_8$). The sample was purchased from Alfa Aesar, ground in a mortar to a fine powder and used without further treatment. Zeolite 13X was purchased from Research Chemicals Ltd., and also used without further treatment.

3. Data processing and sensitivity gain

Figs. 2a and 3a show examples of echo trains induced in andesine and in AL–MSN by the CPMG sequence $(CP)_Y$–$[\tau_{CPMG}$–$(\pi)_Y$–τ_{CPMG}–echo$]_{N_{CPMG}}$ (as shown in Fig. 1a, with $t_1 = 0$). Blanking of the receiver was applied during the π pulses to eliminate the spurious signals associated with high-power RF irradiation. In andesine, the polarization was transferred from the ^{27}Al nuclei, whereas in AL–MSN the initial excitation was applied to protons in the allyl groups. Both samples yielded very long echo trains (see the discussion of transverse dephasing in Section 4), which

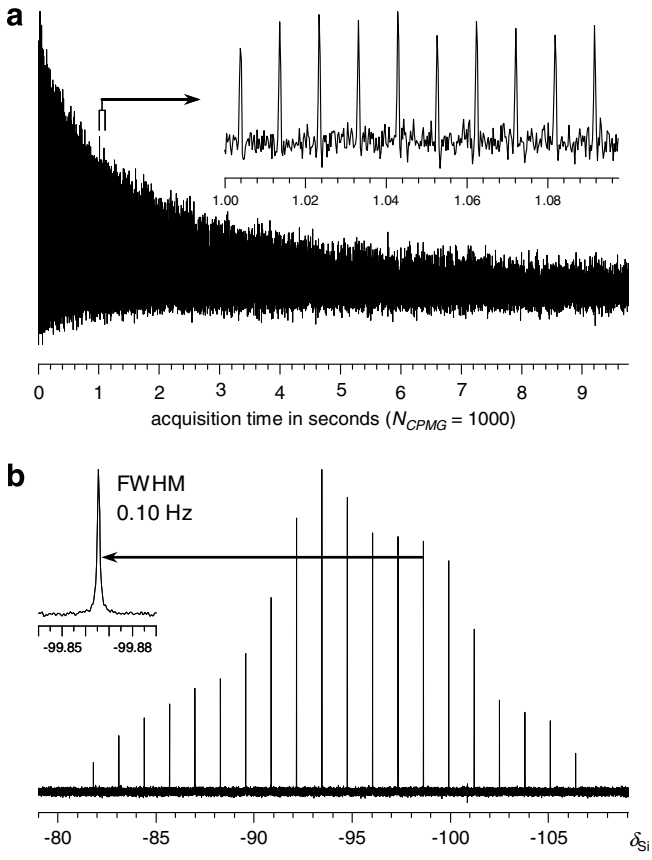

Fig. 2. ^{29}Si spin echoes obtained using CPMG sequence in andesine, acquired with proper blanking of the receiver during the π pulses. (a) The time-domain signal consisting of N_{CPMG} = 1000 echoes (32,016 data points) acquired with ^{29}Si{^{27}Al} CPMAS, under the following experimental conditions: B_0 = 9.4 T, ν_R = 10 kHz, τ_{CP} = 80 ms, ν_{RF}^{Al} = 5.2 kHz during excitation; ν_{RF}^{Al} = 1 kHz during CP, ν_{RF}^{Si} = 11 (±1) kHz during CP (ramped, 11 steps), ν_{RF}^{Si} = 21.6 kHz during π pulses, τ_{CPMG} = 9.75 ms, a delay τ_{RD} between the end of data acquisition and the next scan of 30 ms, and NS = 60. The pulse sequence included RAPT (rotor-assisted population transfer) excitation, which is not shown in Fig. 1a, followed by selective excitation of ^{27}Al central transition. ^{1}H decoupling was not used during data acquisition. Echoes 101 through 110 are shown in the inset. (b) The spikelet spectrum obtained by Fourier transformation of the echo train.

we truncated at N_{CPMG} = 1000 for andesine and N_{CPMG} = 165 for AL–MSN.

A detailed description of CPMG acquisition parameters and data processing has been described earlier [45]. The echoes are generated using intervals $\tau_{CPMG} \approx 5\, T^*_{2,max}$, to allow for the acquisition of the maximum number of echoes per unit time, yet without broadening of any of the spectral lines. In our experiments, these intervals were typically between 5 and 10 ms. The echo trains could be Fourier transformed directly to yield so-called spikelet spectra, as shown in Figs. 2b and 3b. In spite of the truncation, the width of individual ^{29}Si spikelets was only 0.10 Hz in andesine and 0.52 Hz in AL–MSN. Such narrow 'line widths' are exceptionally rare in solid-state NMR spectroscopy. With local field fluctuations being completely frozen, the T_2^{CPMG} times encountered here can exceed those in liquid state.

The CPMG data can also be used to increase the sensitivity of a standard spectrum by superimposing the echoes in the time domain prior to the Fourier transformation. The reconstructed spectrum can be obtained by creating two time-domain signals, composed of the sums of the decaying (right) and rising (left) half-echoes, respectively [45,55]. The first signal, which should also include the initial FID, can be filtered, Fourier transformed and phased in a routine manner. The second one should be inverted

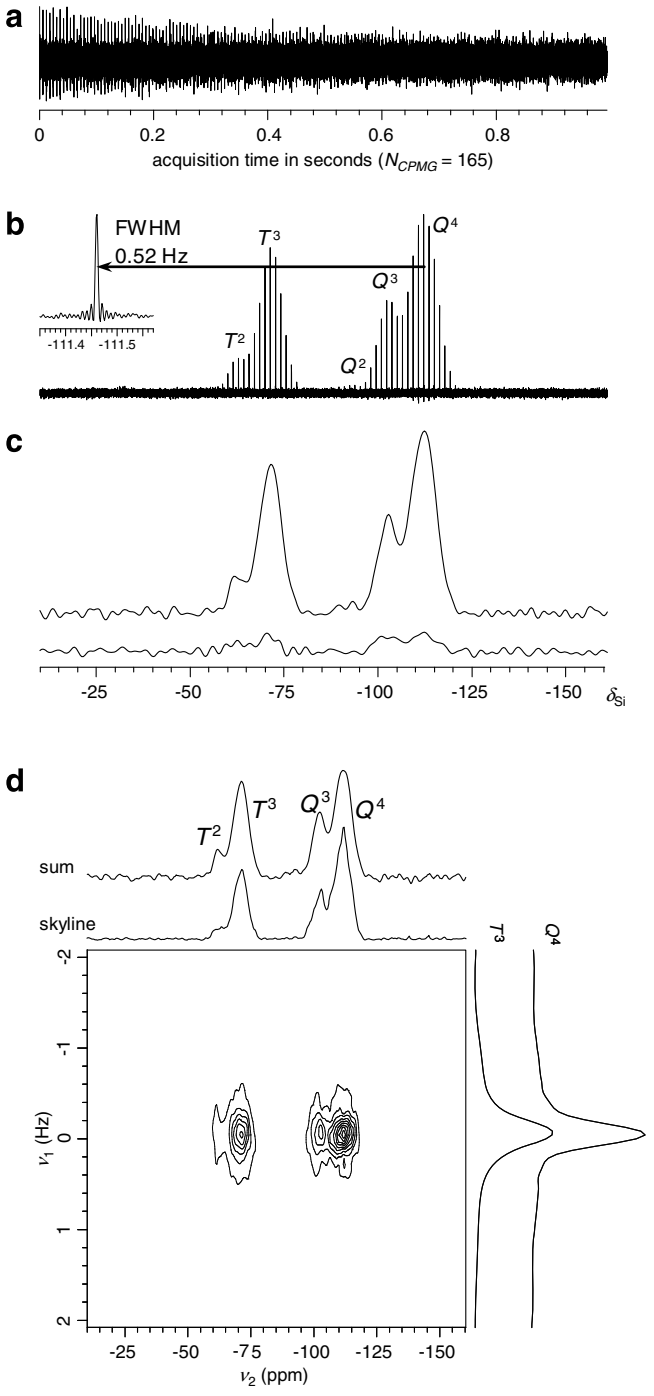

Fig. 3. (a) ^{29}Si spin echoes obtained using the CPMG sequence in functionalized mesoporous silica (AL–MSN), obtained following ^{29}Si{^{1}H} CP: B_0 = 14.1 T, ν_R = 40 kHz, τ_{CP} = 8 ms, ν_{RF}^{H} = 100 kHz during excitation, ν_{RF}^{H} = 60 kHz (±5) kHz during CP (tangent), ν_{RF}^{H} = 12 kHz during SPINAL-64 decoupling, ν_{RF}^{Si} = 100 kHz during CP and π pulses, τ_{CPMG} = 6 ms, N_{CPMG} = 165, τ_{RD} = 0.8 ms, and NS = 320. Three spectra were obtained from this dataset: the spikelet spectrum (b), the reconstructed spectrum (c, top trace), and the 2D T_2^{CPMG}-resolved spectrum (d). The peak assignments are shown in (b), (d). In (c), the reconstructed spectrum is compared with the ordinary spectrum obtained from the first FID. Plotted along the $\nu_1$dimension of the 2D spectrum are the cross sections corresponding to Q^4 and T^3. The sum and skyline projections are compared along ν_2. The inorganic hydrogen in this sample had been exchanged with deuterium, as explained in Section 2.

in time before further processing. The final spectrum is obtained by adding both contributions. The spikelet and reconstructed spectra of AL–MSN derived from the time-domain signal in Fig. 3a are shown in Fig. 3b and c (top trace), respectively. The dramatic in-

crease in sensitivity becomes evident by comparing the reconstructed spectrum with the standard spectrum obtained from the first FID (Fig. 3c, low trace). This scheme can be easily extended to reconstruct 2D spectra, such as ^{29}Si{^{1}H} HETCOR [49,50].

We have shown earlier that the signal enhancement can be expressed as a function of the number of echoes N used for reconstruction of the spectrum [49]

$$G(N) = \frac{1}{\sqrt{2N+1}} \cdot \frac{2 \cdot \exp\left(-(N+1)\frac{\tau_{CPMG}}{T_2^{CPMG}}\right) - \exp\left(-\frac{\tau_{CPMG}}{T_2^{CPMG}}\right) - 1}{\exp\left(-\frac{\tau_{CPMG}}{T_2^{CPMG}}\right) - 1} \quad (1)$$

It has been assumed that the CPMG spectrum includes contributions from all the echoes as well as the initial FID, whose S/N ($G(0)$) was normalized to unity. Eq. (1) has yielded excellent fits to the experimental data measured for all Q^n and T^n silicon sites in functionalized silica materials, with S/N gains exceeding one order of magnitude being achievable [49,50,56]. As will be demonstrated at the end of the Section 4, such remarkable enhancements can be achieved provided that the spin interactions that are not refocusable by the π pulses are eliminated to the greatest extent possible. Fast MAS can be instrumental here, in part because it affords the use of low-power ^{1}H decoupling during long acquisition periods. We note that due to differences in the T_2^{CPMG} values between various sites, $G(N)$ reaches a maximum at different values of N for individual sites. However, the resulting spectral distortions can be minimized by limiting the number of echoes used for the reconstruction (see below).

The CPMG dataset can be also used to construct a 2D time-domain $s(t_1,t_2)$, where all right half-echoes (including the first FID) are separated and aligned as if acquired versus the evolution time $t_1 = N\Delta t_1$ with $\Delta t_1 = \tau_{CPMG}$. A 2D-Fourier transformation of $s(t_1,t_2)$ yields a 'T_2^{CPMG}-resolved' spectrum, with CPMG-narrowed resonances in the ν_1 dimension being separated by the chemical shifts along the ν_2 dimension. The contribution from the left half-echoes is included as well, as in the case of reconstructed ^{29}Si{^{1}H} HETCOR experiment described above. When plotted as a sum 2D projection along ν_2, the resulting ^{29}Si spectrum has enhanced sensitivity and is fully quantitative in nature. An example is shown in Fig. 3d.

4. Transverse dephasing of ^{29}Si nuclei in solids

The origin of surprisingly long transverse dephasing of ^{29}Si nuclei has been recently explored by several research groups [57–59]. These studies mainly targeted crystalline silicon, because of its potential applications in quantum computation. Here, we will briefly summarize the results of the latest study by Ladd et al. [58], in which decoherence time in samples with various contents of ^{29}Si isotope was analyzed by applying multiple pulse sequences and MAS to reverse the dipolar dynamics.

In an isotopically enriched (97%) single-crystal silicon sample, a T_2^{CPMG} of 2 s was observed using the CPMG–MREV-16 × 120 pulse sequence (a homonuclear decoupling sequence based on MREV-16, in which inhomogeneous offsets were periodically refocused by applying π pulses every $120t_c$, with t_c being the duration of the MREV-16 cycle). The T_2^{CPMG} versus t_c dependence showed that decoherence was dominated by second-order terms in the average dipolar Hamiltonian. A T_2^* time of only 450 μs was measured in the same sample following single-pulse excitation. In a similar sample with naturally abundant ^{29}Si, a T_2^{CPMG} of 25 s was observed using the CPMG–MREV–16 × 120 pulse sequence; i.e., the ^{29}Si spins preserved the phase coherence for approximately 10^9 precessional periods [58]. Under the CPMG sequence alone, a T_2^{CPMG} of 11 ms was measured in the same sample. This decay was followed by a long tail lasting several hundred milliseconds, which was also reported in an earlier work and whose origin is not well understood [57]. In an isotopically depleted single crystal sample with approximately 1% of ^{29}Si, a spin echoes decay time of only 8 s was observed under the CPMG–MREV–16 × 120 pulse sequence; its relative 'brevity' was attributed to the presence of lattice defects [58]. In polycrystalline silicon with natural ^{29}Si abundance, the same T_2^{CPMG} value of 8 s was observed under CPMG–MREV–16 × 120, with no dependence on t_c. Under MAS with CPMG, T_2^{CPMG} was a linear function of ν_R (at least in the range 1 kHz $\leqslant \nu_R \leqslant$ 5 kHz used in this study), with the longest value $T_2^{CPMG} = 2.6$ s measured at $\nu_R = 5$ kHz. In summary, it has been concluded that in isotopically enriched and natural single crystals, the decoherence process is dominated by residual dipolar coupling, whereas in polycrystalline samples the T_2^{CPMG} value is limited to 8 s by the magnetic fluctuations induced by impurities (the so-called 1/f noise [60]) at silicon surfaces [58].

Although detailing the mechanism of transverse dephasing was not the goal of this report, we explored the effect of various experimental strategies on the coherence lifetime in samples of our interest. To this end, we measured the spin–echo trains in AL–MSN as a function of ν_R, both with and without ^{1}H decoupling using SPINAL-64 [61]. Prior to Fourier transformation the echoes were co-added to produce the reconstructed spectra. The S/N gain G was then measured as a function of the number of echoes N for all individual sites in this sample. The results shown in Fig. 4 are representative of sites that are isolated (Q^4, Fig. 4a) and in the proximity of hydrogen (T^3, Fig. 4b). Similar curves have been obtained for Q^2, Q^3 and T^2 sites (not shown). As demonstrated in Fig. 4, these data could be fitted using Eq. (1), using T_2^{CPMG} as the only variable parameter. The results are given in Table 1 along with the transverse dephasing times T_2^{HE} measured using the rotor-synchronized Hahn echo sequence $(CP)_Y$–τ –$(\pi)_Y$–τ. This sequence removes contributions from magnetic field inhomogeneity, magnetic susceptibility and the distribution of chemical shifts, but has minimal effect on heteronuclear dipolar interactions and no effect on homonuclear dipolar dephasing.

We first note that in the absence of homonuclear decoupling the dephasing due to ^{29}Si–^{29}Si dipolar interaction is expected to be on the order of 50 ms in naturally abundant silica. This implies that in all measurements performed under the static condition the decoherence was mainly due to heteronuclear dipolar interaction with protons. When neither MAS nor ^{1}H decoupling was used, the T_2^{HE} times (0.6–0.9 ms) were only slightly longer than T_2^* (~0.2 ms). The ^{1}H decoupling extended the T_2^{HE} by approximately one order of magnitude. The use of the CPMG sequence instead of a single π pulse further increased the decoherence time, to 5–12 ms in the absence of ^{1}H decoupling and to 10–20 ms with ^{1}H decoupling. The CPMG refocusing averages out the inhomogeneous terms of the broadening Hamiltonian, which are linear in the observed spins' I_z operator and which do not fluctuate during the period τ_{CPMG} [20]. Thus, with $\tau_{CPMG} = 6$ ms, the dephasings due to ^{29}Si–^{29}Si interactions and (in the absence of ^{1}H decoupling) ^{1}H–^{29}Si interactions become partly refocused.

To facilitate the discussion of results obtained under MAS, we note that the T_2^{CPMG} values were measured without ^{1}H decoupling for $\nu_R = 10$, 25 and 40 kHz, whereas ^{1}H decoupling was only used under fast MAS ($\nu_R = 40$ kHz). This was necessary because at the lower MAS rates, efficient heteronuclear decoupling required the use of high-RF magnetic field strength, which exceeded ν_R by a factor of at least 3 [62]. With acquisition times approaching 1 s, high power could not be safely dissipated within the probe. Under MAS at 40 kHz, however, efficient heteronuclear decoupling could be easily achieved by using low-RF field strength corresponding to a precession frequency much smaller than ν_R [49,63].

MAS can average out the interactions leading to inhomogeneous line broadening as well as the homogeneous dipolar effects (to zero

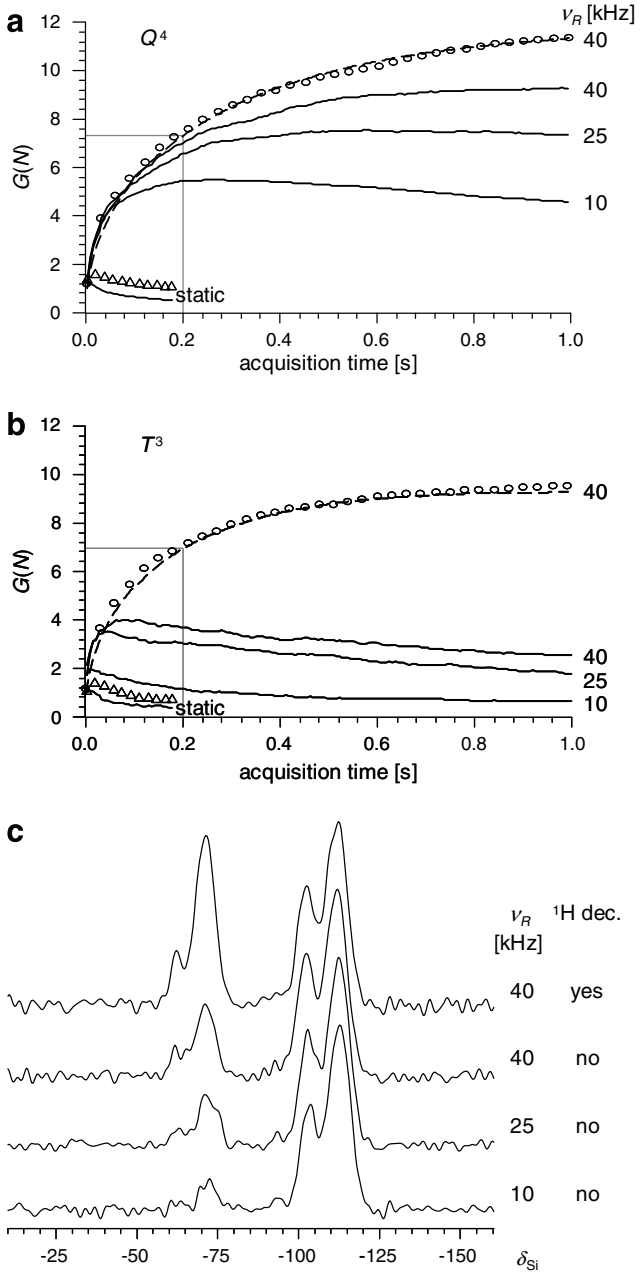

Fig. 4. Sensitivity gain as a function of N ($0 \leqslant N \leqslant N_{CPMG}$) for Q^4 sites (a) and T^3 sites (b) in AL–MSN, measured in a static sample ($\nu_R = 0$, $N_{CPMG} = 30$) and under MAS ($\nu_R = 10$, 25 and 40 kHz; $N_{CPMG} = 165$). Solid lines represent data obtained without ^{1}H decoupling. SPINAL-64 ^{1}H decoupling was applied under static condition (using $\nu_{RF}^H = 25$ kHz, triangles) and under 40 kHz MAS (with $\nu_{RF}^H = 12$ kHz, circles). Other experimental conditions were as given in the caption to Fig. 3a. The quality of fits obtained using Eq. (1) is demonstrated for data obtained under 40 kHz MAS and SPINAL-64 decoupling (dashed lines). (c) Examples of spectra reconstructed using $N = 33$ under different experimental conditions.

in the zeroth order, whereas higher order corrections are still present). At the lowest MAS rate used ($\nu_R = 10$ kHz), the modulation of dipolar interactions was already faster than that in the case of CPMG alone, as indeed reflected by the increased T_2^{CPMG} values, which reached 250 ms for Q^4 sites. As expected, the T_2^{CPMG} values measured for all Q^n and T^n sites are roughly proportional to ν_R [62]. However, for sites T^2 and T^3 MAS alone is powerless in refocusing ^{29}Si magnetization for an extended period of time, even at 40 kHz, due to more rapid dephasing of their magnetization by the residual dipolar couplings with protons in allyl groups. Only by combining 40 kHz MAS and low-power ^{1}H decoupling could long-lived trains of spin echoes be generated for all sites. We have not established the relative contributions of homo- and heteronuclear interactions to the largest T_2^{CPMG} value found under these conditions (900 ms in Q^4 sites). However, the observed difference in T_2^{CPMG} values between Q^4 sites and the most protonated sites in AL–MSN (T^2 and Q^2) indicates that better averaging of ^{1}H–^{29}Si interactions is still possible by using faster MAS and/or decoupling sequences designed specifically to increase the coherence lifetime [64].

Table 1
Transverse dephasing times T_2^{HE} and T_2^{CPMG} (ms) measured for T^n and Q^n sites in an AL–MSN sample under various MAS (ν_R, kHz) and ^{1}H decoupling (ν_{RF}^H, kHz) conditions

	Experimental conditions		Silicon site				
	ν_R	ν_{RF}^H	T^2	T^3	Q^2	Q^3	Q^4
T_2^{HE}	0	0	0.8	0.9	0.6	0.7	0.9
	0	25	7.0	6.5	7.0	9.0	12.0
	40	0	50	25	–	80	100
	40	12	60	90	–	200	120
T_2^{CPMG}	0	0	5	7	4	7	12
	0	25	20	15	10	15	20
	10	0	20	50	–	150	250
	25	0	60	80	–	300	450
	40	0	200	130	–	400	600
	40	12	420	650	350	500	900

Under MAS, the T_2^{CPMG} values were obtained by fitting the $G(N)$ curves using Eq. (1). Static data were fitted directly using the echo trains.

The $G(N)$ values observed in mesoporous silicas under 40 kHz MAS and ^{1}H decoupling are remarkably high. Indeed, for Q^4 sites in AL–MSN, a sensitivity gain exceeding one order of magnitude can be achieved by utilizing all available echoes (Fig. 4a). Due to shorter T_2^{CPMG} time, the gain is noticeably lower for T^3 sites in the same sample (Fig. 4b). However, the dependence of signal enhancement on T_2^{CPMG} could be practically eliminated by reducing the number N of echoes used for reconstruction. In the case of AL–MSN, by limiting N to 33 (which corresponds to an acquisition time of ~200 ms, as marked in Fig. 4a and b), the S/N gain for all sites is between 6.9 and 7.2; i.e., the resulting spectra are quantitative to within a few percent. In other samples of our interest, sensitivity gains on the order of 3–10 could be typically obtained under similar conditions while accurate relative intensities were maintained (see below) [49,50]. The effect of MAS and ^{1}H decoupling is evident in Fig. 4c, which shows four spectra reconstructed using the same number of echoes ($N = 33$). Clearly, slower MAS and lack of decoupling discriminate silicon sites with stronger coupling to protons from other silicon sites.

5. ^{29}Si NMR spectroscopy with CPMG acquisition

Recent studies performed in our laboratory have demonstrated that sensitivity gains described in previous sections can be projected onto various 1D and 2D ^{29}Si NMR experiments involving mesoporous silicas, zeolites, and other inorganic materials.

5.1. ^{29}Si{^{1}H} HETCOR NMR of functionalized mesoporous silica materials

The structures of organic–inorganic interfaces are best probed using the 2D ^{29}Si{^{1}H} HETCOR NMR method, which determines the location of organic groups relative to various silicon sites. However, such experiments usually require acquisition times on the order of days, even in studies of hydrogen-rich interfaces between a silica surface and a surfactant [10,11]. Most of our recent studies have focused on functionalized silica surfaces from which the surfactant species were previously removed [49,50,54]. In several cases the organic content of such samples was below the sensitivity limit of the

'standard' $^{29}Si\{^1H\}$ HETCOR method, yet such an examination became possible by implementing the CPMG refocusing. Two examples of the reconstructed versions of such spectra measured in AL–MSN and CMTES–MSN are shown in Figs. 5 and 6.

Interestingly, strong cross peaks were observed between Q^4 silicon sites and hydrogens H2 and H3 in AL–MSN. These cross peaks result from spatial proximity rather than ^1H–^1H spin diffusion. Thus, some of the allyl groups appear to be in a prone orientation with respect to the silica surface [65]. A similar spectrum of this sample has been earlier acquired at a lower magnetic field (9.4 T) [49].

We previously used the spectrum of CMTES–MSN (Fig. 6a) as part of our studies of covalent linkages formed during organic functionalization of MCM-41 silica with chloroalkylsilanes [50]. The ^1H cross sections shown in Fig. 6b correspond to silicon sites in the '*T*' range, which are directly bound to one carbon. By correlating the ^1H traces with the corresponding $^{13}C\{^1H\}$ HETCOR spectrum, it has been shown that ^{29}Si resonances at −77 and −80 ppm, labeled T^3_A and T^3_B, correspond to $(\equiv SiO)_3\mathbf{Si}(CH_2Cl)$. Very different ^1H traces are observed at −66 ppm (T^2_A), −69 ppm (T^2_B) and −73 ppm (T^2_C), which represent $(\equiv SiO)_2\mathbf{Si}(CH_2Cl)(OCH_2CH_3)$ sites bound to both CH_2Cl and ethoxy groups [50]. The Q^3 and Q^4 sites in CMTES–MSN are correlated with ^1H resonances representing the attached functionalities and the hydrogen bonded species $\equiv Si–OH–(H_2O)_n$ (note that this sample was studied in non-deuterated state). An unexpected caveat associated with this spectrum is the discrepancy between traces reconstructed using two different sections of the echo train. This can be best illustrated by analyzing the 1D $^{29}Si\{^1H\}$ dataset, acquired with more scans. Trace 1 in Fig. 6c represents the first FID and echoes 1 through 6, whereas the tail of the echo train (echoes 140 through 160) was used to create trace 2. There is a clear change in resolution between the traces, which must be attributed to the heretofore unidentified distribution of T_2^{CPMG} times associated with individual silicon sites. Evidently, the signals that contribute to trace 2 represent sites with increasingly longer T_2^{CPMG} and narrower T^2 and T^3 resonances. This may be associated with the existence of sample regions with various degrees of local order [2].

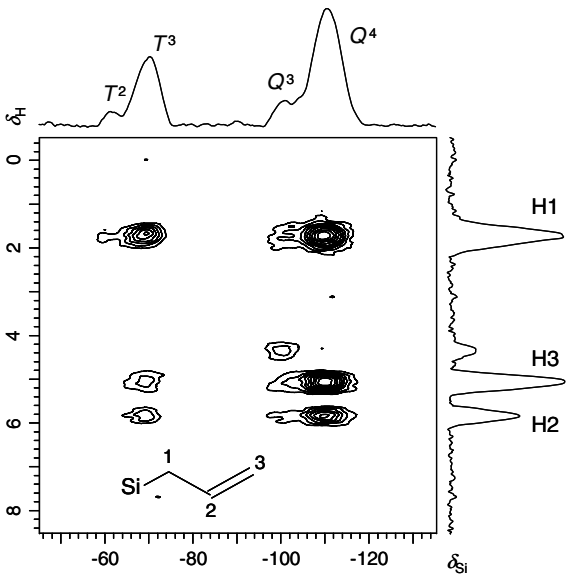

Fig. 5. $^{29}Si\{^1H\}$ HETCOR spectrum obtained in AL–MSN silica using following conditions: B_0 = 14.1 T, ν_R = 40 kHz, τ_{CP} = 8 ms, $\nu^H_{RF} = 208$ kHz during excitation, $\nu^H_{RF} = 130 \pm 5$ kHz during CP (ramped), $\nu^H_{RF} = 12$ kHz during TPPM decoupling, $\nu^{Si}_{RF} = 90$ kHz during CP and CPMG pulses, N_{CPMG} = 124, τ_{CPMG} = 4 ms, τ_{RD} = 0.8 s, and NS = 200; and 80 increments of 100-μs were used in the t_1 dimension. The total experimental time was 12 h. The inorganic hydrogen in this sample had been exchanged with deuterium, as explained in Section 2.

The question arises to what extent the above approach to measuring 2D $^{29}Si\{^1H\}$ spectra under fast MAS offers an advantage over the traditional method utilizing slower spinner and multiple pulse ^1H decoupling (e.g., FSLG), assuming that both experiments are performed with CPMG refocusing. The benefits of using fast MAS include better sensitivity per spin, lack of spinning sidebands, lack of a scaling factor in the ^1H dimension, the accessibility of low-power decoupling schemes and simple experimental setup. Whereas larger rotor can accommodate more sample, its volume has to be restricted because of stringent requirements of multiple pulse ^1H decoupling on the RF magnetic field homogeneity. For example, in our earlier $^{13}C\{^1H\}$ HETCOR experiments with 5 mm rotors we used only one third (∼50 μL) of the available rotor capacity to avoid degrading the ^1H resolution. The CP efficiency is more difficult to compare, as it also depends on RF circuitry (especially the coil design) and may vary from sample to sample. Our evaluation of $^{13}C\{^1H\}$ HETCOR strategies in mesoporous catalysts, performed without the CPMG acquisition, showed that the fast MAS approach yielded spectra of similar sensitivity and resolution than those obtained in a 5-mm rotor using FSLG ^1H decoupling [49]. A reasonable albeit untested expectation is that the sensitivities would behave similarly in the case of 2D $^{29}Si\{^1H\}$ NMR. Since, as shown in Section 4, the CPMG detection performs better under high spinning rates, the overall benefits of using fast MAS in such experiments outweigh the sensitivity gain due to high sample volume. It should be noted that until now our experience with such experiments has been limited to samples in which MAS at 40 kHz can provide sufficient ^1H homonuclear decoupling. There is considerable interest in the development of RF sequences for high resolution ^1H spectroscopy under fast MAS, which can make the CPMG approach even more attractive.

5.2. Quantitative ^{29}Si DPMAS measurements

Whereas there is a clear advantage of using the CPMG refocusing under fast MAS in the context of $^{29}Si\{^1H\}$ HETCOR, the usefulness of such strategy for acquisition of quantitative 1D ^{29}Si DPMAS spectra is more difficult to assess. We compared the CPMG method with the long-established approach of measuring a single FID in a larger (5 mm) rotor, under the criterion that spectra must be quantitative to within 5%. As described earlier (Section 4), in deuterated AL–MSN the S/N ratio could be increased sevenfold (with N = 33, Fig. 4a and b) under fast MAS. A similar measurement performed on this sample in a 5-mm rotor (fully loaded with the studied material, under 8 kHz MAS and 30 kHz TPPM ^1H decoupling) yielded the same S/N ratio per scan with N = 0 (the first FID). We found this result to be typical of other functionalized silica materials. In cases when 'good' (i.e., quantitative) echoes can be acquired at low MAS rate, large volume rotors provide undistorted DPMAS spectra with best overall sensitivity. We found the number of such echoes to be typically between 1 and 5. This number was generally higher in samples that were deuterated and/or dried prior to the measurement.

5.3. $^{29}Si\{^{27}Al\}$ HETCOR NMR of zeolite 13X

Heteronuclear $^{29}Si\{^{27}Al\}$ NMR spectra, if routinely available, would be extremely helpful in studies of aluminosilicates. However, such experiments are inherently challenging due to the low efficiency of the CP process involving quadrupolar nuclei [66,67] and low concentrations of ^{27}Al–^{29}Si spin pairs, especially in materials with high Si/Al ratios. The feasibility of $^{29}Si\{^{27}Al\}$ NMR methods has nevertheless been demonstrated in 1D and 2D studies of zeolites [68], minerals [69], and ceramic materials [70]. In the latter study, the sensitivity was enhanced by increasing the population inversion across the central transition using RAPT [71]. More

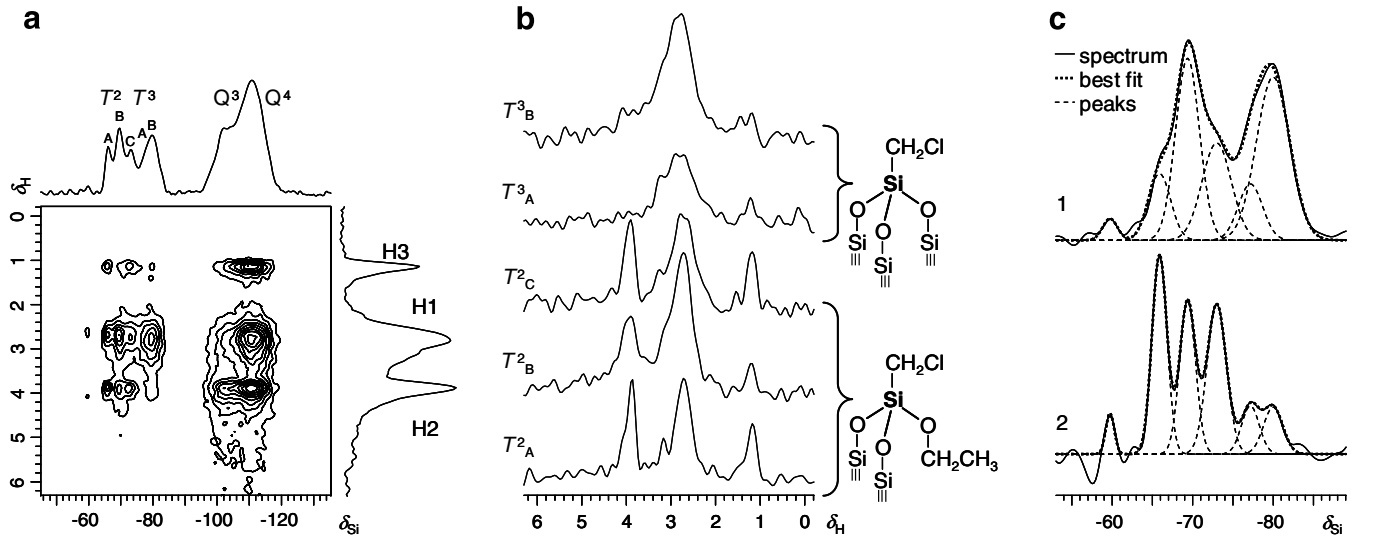

Fig. 6. $^{29}Si\{^1H\}$ experiments on CMTES–MSN. (a) $^{29}Si\{^1H\}$ HETCOR: B_0 = 14.1 T, ν_R = 25 kHz, τ_{CP} = 8 ms, ν_{RF}^H = 104 kHz during excitation, ν_{RF}^H = 30 ± 3 kHz during CP (ramped), ν_{RF}^H = 6 kHz during TPPM decoupling, ν_{RF}^{Si} = 55 kHz during CP and CPMG pulses, N_{CPMG} = 160, τ_{CPMG} = 6 ms, τ_{RD} = 1 s, and NS = 80; and 100 increments of 80-μs were used in the t_1 dimension. The total experimental time was 9 h. (b) Cross-sections along the ^1H dimension corresponding to T^2 and T^3 sites. (c) ^{29}Si spectra of T^n sites reconstructed from 1D $^{29}Si\{^1H\}$ echo train using echoes 1 through 6 (top) and 140 through 160 (bottom). Experimental conditions were the same as in (a) except for NS, which was set to 1280.

recently, the isotropically resolved $^{29}Si\{^{27}Al\}$ HETCOR spectrum of the mineral microcline ($KAlSi_3O_8$) has been recorded by combining RAPT-CPMAS and SPAM-MQMAS methods [72].

The CPMG acquisition of $^{29}Si\{^{27}Al\}$ spectra is less likely to yield the overall sensitivity gains achieved in $^{29}Si\{^1H\}$ NMR. First, the T_1 relaxation of ^{27}Al nuclei is usually very fast, which allows for the use of short recycle delays. However, even when the recycle delay (defined as the interval between the completion of FID detection and the start of the next pulse sequence) can be as short as 10 ms, the overall cycle time of the experiment (defined as the interval between analogous points of successive pulse sequences) is prolonged considerably by the RAPT sequence, the t_1 evolution and the CP period. Thus, the CPMG refocusing can still offer an advantage because it extends the cycle time by only a few ms per echo. Second, several conflicting factors have to be considered while optimizing the experimental strategy for cross polarization and decoupling. The spin dynamics during CP generally favors the use of fast MAS, under the so-called sudden passage condition [66,67,73]. Similarly, ^{27}Al decoupling should be more effective under fast MAS. Indeed, under slow MAS conditions the spin echoes are likely to be attenuated due to the recoupling of the ^{29}Si–^{27}Al dipolar interaction as a result of adiabatic transfer of populations among the ^{27}Al Zeeman states (TRAPDOR effect) [74,75]. The spin dynamics involved in these processes depends on the quadrupole parameters and resonance offsets, and has complex orientational anisotropy. On the other hand, the CPMG refocusing in our $^{29}Si\{^{27}Al\}$ experiments has not been strongly influenced by ^1H decoupling. With extended ^1H irradiation no longer needed, the use of larger MAS rotors may become advantageous.

In spite of these complexities, the CPMG proved very helpful in $^{29}Si\{^{27}Al\}$ experiments. In Fig. 7 we show an example of a $^{29}Si\{^{27}Al\}$ HETCOR spectrum of zeolite 13X, which exhibits connectivities between tetrahedral aluminum sites (labeled Al_1^{IV} and Al_2^{IV}) and Q^4 sites associated with three and four Al neighbors (labeled Q_3^4 and Q_4^4, respectively). We are not aware of earlier reports that would show the existence of different Al^{IV} sites in this zeolite. By using a moderate MAS rate (8 kHz) and three CPMG echoes, we were able to boost the sensitivity by a factor of ~2, which was further doubled by RAPT. Similar gains were achieved in the recently reported studies of mesoporous aluminum silicate catalysts [76]

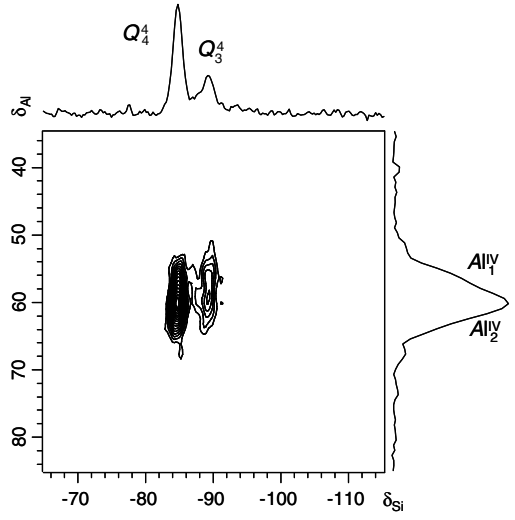

Fig. 7. $^{29}Si\{^{27}Al\}$ HETCOR-CPMG spectrum of zeolite 13X: B_0 = 9.4 T, ν_R = 8 kHz (5 mm rotor), τ_{CP} = 6 ms, ν_{RF}^{Al} = 5.2 kHz during RAPT (with modulation frequency of 167 kHz and duration of 1.4 ms), ν_{RF}^{Al} = 5.2 kHz during excitation, ν_{RF}^{Al} = 1 kHz during CP, ν_{RF}^{Si} = 11 (±1) kHz during CP (ramped, 11 steps), ν_{RF}^{Si} = 21.6 kHz during CPMG pulses, N_{CPMG} = 3, τ_{CPMG} = 6 ms, τ_{RD} = 12 ms, and NS = 16,000; and 50 increments of 50-μs were used in the t_1 dimension. The total experimental time was 18 h.

and in synthetic zeolite ZSM-4 [77], where new and unexpected correlations were observed between different components of ^{29}Si and ^{27}Al spectra. We have not performed extensive optimizations of these experiments; it is quite likely that further improvements can be made.

5.4. ^{29}Si–^{29}Si DQMAS homonuclear correlation NMR of mesoporous silica

Another potential application of CPMG refocusing is in DQMAS ^{29}Si–^{29}Si NMR. DQ filtering eliminates the dominant single quantum (SQ) coherences from isolated ^{29}Si spins, which simplifies the spectra, especially in naturally abundant samples. The DQ

coherences can be created and reconverted under MAS by using dipolar recoupling methods, such as BABA [78] and C7 [79], or by using isotropic J-couplings (via bridging oxygen atoms, ^{29}Si–O–^{29}Si) in the INADEQUATE experiment [51]. Since the dipolar coupling constants in ^{29}Si–O–^{29}Si pairs (~160 Hz) are larger than the corresponding $^2J_{\mathrm{Si-Si}}$ couplings (typically 5–15 Hz) [52,80,81], the dipolar recoupling sequences lead to much faster coherence build-up [15]. The utility of both approaches has been demonstrated in several studies of naturally abundant silicates and aluminosilicates, including zeolite ZSM-5 [16], zeolites ZSM-12 and KZ-2 [52], highly ordered mesostructured silicas [11,17] and clathrasil [15]. Due to their well-ordered structure, these materials exhibited relatively narrow ^{29}Si resonances, ranging between 0.2 and 1.5 ppm (FWHM). The MSN materials of interest to us are highly amorphous, leading to considerably wider distribution of local environments. The resulting broadening of ^{29}Si lines (typically 5–8 ppm for any given type of site) affects both SQ and DQ dimensions of 2D spectra, thereby posing a sensitivity challenge.

Most important for CPMG refocusing of DQ-filtered ^{29}Si coherences is that they usually involve chemically bound nuclei experiencing homonuclear $^2J_{\mathrm{Si-Si}}$ coupling. For example, all nuclei contributing to INADEQUATE spectra of MSNs are coupled through ^{29}Si–O–^{29}Si bridges. This coupling is not refocused by the π pulses, which results in modulation of the observed CPMG echoes. In addition, the decay time of the echo train can decrease due to distribution of the J-coupling values. This limits the number of echoes available for reconstruction using the scheme proposed above. With extended ^{1}H decoupling being unnecessary, the use of MAS rotors with larger volume becomes advantageous in such experiments. We note that in INADEQUATE experiments with disordered samples this argument may be outweighed by the need to spin fast in order to minimize the losses during coherence transfers. Indeed, there are well-known benefits of using the refocused version of the INADEQUATE experiment in samples with a short time constant T_2^* [53]. Using fast MAS should slow down the T_2^{HE} dephasing, and thus reduce the loss of ^{29}Si magnetization during time delays τ_1 and τ_2 (see Fig. 1b).

An example of a ^{29}Si–^{29}Si{^{1}H} refocused INADEQUATE spectrum of an MSN sample acquired with CPMG detection is shown in Fig. 8a. Due to modulation by J-coupling, only the first four out of 10 acquired echoes were used for reconstruction, which limited the sensitivity gain to ~2.5. Still, the Q^3–Q^4, Q^3–Q^3 and Q^4–Q^4 correlations are clearly identified.

The modulation of the DQ-filtered train of CPMG echoes is evident in the spikelet spectrum obtained via Fourier transformation of the entire echo train (not shown). The individual spikelets include two main components separated by the mean value of the scalar couplings between ^{29}Si nuclei. More detailed insights can be gained by measuring the first row of ^{29}Si–^{29}Si{^{1}H} refocused INADEQUATE spectrum and constructing a new time domain $s(t_1,t_2)$ in which the half-echoes are aligned along t_1, where $t_1 = N\tau_{\mathrm{CPMG}}$ ($1 \leqslant N \leqslant N_{\mathrm{CPMG}}$), as explained in the end of Section 3. After 2D-Fourier transformation one obtains the DQ-filtered and J-resolved spectrum shown in Fig. 8b. In this case, we used $N_{\mathrm{CPMG}} = 50$, in order to include the entire J-evolution. The theoretical principles of spin-echo modulation, as a function of echo duration, due to homonuclear J-couplings in isolated pairs of spin-1/2 nuclei under MAS were scrutinized in a recent study by Duma et al. [82]. The modulation depends on the degree of magnetic equivalence, chemical shift anisotropy (CSA) parameters, strength of dipolar interactions, relative orientation between the dipolar and CSA tensors, and experimental conditions (ν_{R}). In short, two major modulation regimes were described: regime A, in which J-modulation is small or absent, observed under fast MAS in pairs of nuclei with very similar CSA parameters; and regime B, in which the J-modulated component is dominant, observed under moderate ν_{R} in the presence of dipolar coupling and/or CSA, especially in spin pairs with different isotropic chemical shifts [82].

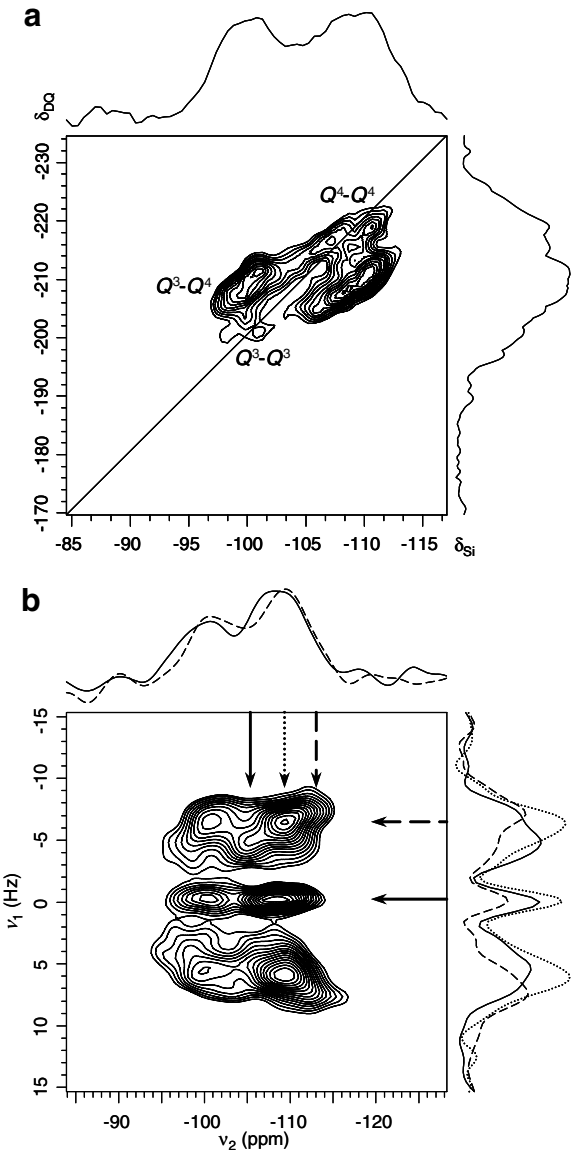

Fig. 8. (a) ^{29}Si–^{29}Si{^{1}H} refocused INADEQUATE spectra of MSN: $B_0 = 9.4$ T, $\nu_{\mathrm{R}} = 8$ kHz (5 mm rotor), $\tau_{\mathrm{CP}} = 12$ ms, $\nu = 71$ kHz during excitation, $\nu_{\mathrm{RF}}^{\mathrm{H}} = 52 \pm 3$ kHz during CP (ramped, 11 steps), $\nu_{\mathrm{RF}}^{\mathrm{H}} = 35$ kHz during TPPM decoupling, $\nu_{\mathrm{RF}}^{\mathrm{Si}} = 44$ kHz during CP, $\nu_{\mathrm{RF}}^{\mathrm{Si}} = 50$ kHz during CPMG pulses, $\tau_1 = \tau_2 = 15$ ms, $N_{\mathrm{CPMG}} = 10$ (only four echoes were used to generate the spectrum), $\tau_{\mathrm{CPMG}} = 10.125$ ms, $\tau_{\mathrm{RD}} = 1.2$ s, and NS = 2560; and 82 increments of 250-μs were used in the t_1 dimension. The total experimental time was 60 h. The J-resolved spectrum (b) was obtained by measuring the first row of INADEQUATE spectrum ($t_1 = 0$) with $N_{\mathrm{CPMG}} = 50$ and NS = 320, under otherwise the same conditions. The 2D spectrum was obtained by rearranging all echoes to produce a second time-domain, as explained in the text. The line styles used in the cross sections correspond to the arrows on the spectrum.

Our experiments showed that the modulation generated by a CPMG train of π pulses is additionally sensitive to the length of the τ_{CPMG} period (with rotor synchronization being always used). Whereas further studies are necessary to better understand and exploit the spin dynamics in these experiments, several remarks can be made. First, Fig. 8b shows that for most spins the observed modulation is indeed dominated by $^2J_{\mathrm{Si-Si}}$ couplings. Most likely, these resonances correspond to what Duma et al. [82] referred to as regime B, i.e., spin pairs with different chemical shifts (i.e., $^2J_{\mathrm{Si-Si}}$ couplings between Q^4 and Q^3 sites). The width of the 2D spectrum in the ν_1 dimension can be attributed at least in part to the distribu-

tion of J values. Indeed, there is a noticeable correlation between $^2J_{Si-Si}$ couplings and the corresponding chemical shifts. For example, the more shielded Q^4 sites (at around −113 ppm) have $^2J_{Si-Si}$ values of ∼14 Hz, whereas Q^4 resonances at −105 ppm have $^2J_{Si-Si}$ values centered at 10 Hz (the corresponding cross sections are shown in Fig. 8b, right). These values can be associated with the mean Si–O–Si bond angles [81]. It has been recently shown that conditional probability distributions of chemical shifts can be extracted from 2D INADEQUATE spectra [83]. Although, it is not yet clear to what extent the widths of individual cross sections along ν_1 are due to the distribution of $^2J_{Si-Si}$ values, similar analysis of the spectrum in Fig. 8b may provide a new source of information about structural disorder in silica materials. Second, there is a considerable fraction of spins for which the modulation is quenched. These resonances may be due to Q^4–Q^4 and Q^3–Q^3 pairs with similar shifts (regime A) (Note that truly magnetically equivalent spins should not be observed in the INADEQUATE experiment). Another possible origin of the central peak is the contribution from isolated non-coupled ^{29}Si spins due to incomplete DQ filtering.

6. Conclusions

We have evaluated the uselessness of CPMG refocusing in the context of several ^{29}Si NMR techniques and analyzed the strategies that maximize the sensitivity. The greatest utility of CPMG refocusing was found in CP-based ^{29}Si{^{1}H} HETCOR experiments performed under fast MAS on functionalized mesoporous silicas. The examples of such spectra shown here are representative of numerous materials studied recently in our laboratory, for which remarkable sensitivity gains have been achieved without creating excessive spectral distortions. The ^{29}Si{^{1}H} HETCOR spectra, which under standard conditions would be prohibitively time consuming to acquire, were measured in less than a day. We achieved similar enhancements in ^{29}Si{^{19}F} HETCOR experiments.

^{29}Si DPMAS spectra can be also enhanced by CPMG acquisition, although the number of echoes must be carefully controlled if quantitative accuracy is to be preserved. Typically, the use of CPMG under fast MAS can roughly make up for the loss of intensity due to smaller rotor size. Drying of the sample or exchange of protons in H_2O and OH groups with deuterium usually permits the use of CPMG echoes in high volume rotors, providing the highest overall sensitivity.

The best strategies for ^{29}Si{^{27}Al} CPMAS and ^{29}Si–^{29}Si INADEQUATE CPMG experiments are less clear-cut. In our ^{29}Si{^{27}Al} measurements, ^{1}H decoupling did not significantly affect the refocusing. Whereas polycrystalline andesine yielded 1000 echoes in a 10-s train, the mesoporous aluminum silicates and zeolites typically produced only a few echoes, even under fast MAS and ^{1}H decoupling. When ^{1}H decoupling is not needed, the use of larger MAS rotors becomes advantageous. On the other hand, ^{29}Si{^{27}Al} CP and ^{27}Al decoupling may favor fast MAS. The efficiency of our ^{29}Si{^{27}Al} experiments, which were mostly performed with 5 mm rotors under 8–10 kHz MAS, was at least doubled by CPMG refocusing. Fast T_1 relaxation of ^{27}Al nuclei allowed for acquisition of 2D spectra in some of the samples within a day. Better decoupling methods, including double ^{1}H and ^{27}Al decoupling, need to be explored. The DQ-filtered ^{29}Si–^{29}Si experiments can also benefit from CPMG acquisition. In this case the echoes are modulated by $^2J_{Si-Si}$ coupling, which can be exploited in J spectroscopy. Again, further studies are needed to assess the utility of fast MAS in studying homonuclear silicon–silicon correlations.

Acknowledgments

This research at the Ames Laboratory was supported by the U.S. Department of Energy, Office of Basic Energy Sciences, under Contract No. DE-AC02-07CH11358. The authors are indebted to Drs. Z. Gan and G. J. Kennedy, for helpful discussions, and to Dr. J. Rapp and K. Mao for assistance with some of the measurements. The sample of CMTES–MSN was kindly provided by Drs. S. Ganapathy and S. Bhaduri.

References

[1] G. Engelhardt, D. Michel, High-resolution Solid-state NMR of Silicates and Zeolites, John Wiley and Sons, Chichester, 1987 (Chapters 3–6).
[2] G.E. Maciel, Solid-state NMR spectroscopy of inorganic materials, in: J.J. Fitzgerald (Ed.), ACS Symposium Series 717, American Chemical Society, Washington, DC, 1999, pp. 326–356.
[3] M.A. Petrich, Amorphous silicon alloys, in: D.M. Grant, R.K. Harris (Eds.), Encyclopedia of Nuclear Magnetic Resonance, John Wiley and Sons, Chichester, 1996, pp. 779–789.
[4] R. Dupree, Ceramics, in: D.M. Grant, R.K. Harris (Eds.), Encyclopedia of Nuclear Magnetic Resonance, John Wiley and Sons, Chichester, 1996, pp. 1222–1225.
[5] H. Eckert, Structural characterization of noncrystalline solids and glasses using solid state NMR, Prog. NMR Spectrosc. 24 (1992) 159–293.
[6] Y. Takeuchi, T. Takayama, ^{29}Si NMR spectroscopy of organosilicon compounds, Chem. Org. Silicon Comp. 2 (1998) 267–354.
[7] S. Kuroki, H. Kimura, I. Ando, Structural characterization of Si-based polymer materials by solid-state NMR spectroscopy, Ann. Rep. NMR Spectrosc. 52 (2004) 201–243.
[8] N.A. Melosh, P. Lipic, F.S. Bates, F. Wudl, G.D. Stucky, G.H. Fredrickson, B.F. Chmelka, Molecular and mesoscopic structures of transparent block copolymer–silica monoliths, Macromolecules 32 (1999) 4332–4342.
[9] J. Brus, M. Spirkova, D. Hlavata, A. Strachota, Self-organization, structure, dynamic properties, and surface morphology of silica/epoxy films as seen by solid-state NMR, SAXS, and AFM, Macromolecules 37 (2004) 1346–1357.
[10] N. Baccile, G. Laurent, C. Bonhomme, P. Innocenzi, F. Babonneau, Solid-state NMR characterization of the surfactant–silica interface in templated silicas: acidic versus basic conditions, Chem. Mater. 19 (2007) 1343–1354.
[11] S.C. Christiansen, D. Zhao, M.T. Janicke, C.C. Landry, G.D. Stucky, B.F. Chmelka, Molecularly ordered inorganic frameworks in layered silicate surfactant mesophases, J. Am. Chem. Soc. 123 (2001) 4519–4529.
[12] A.J. Vega, Heteronuclear chemical-shift correlations of silanol groups studied by two-dimensional cross-polarization magic angle spinning NMR, J. Am. Chem. Soc. 110 (1988) 1049–1054.
[13] C.A. Fyfe, Y. Zhang, P. Aroca, An alternative preparation of organofunctionalized silica gels and their characterization by two-dimensional high-resolution solid-state heteronuclear NMR correlation spectroscopy, J. Am. Chem. Soc. 114 (1992) 3252–3255.
[14] M.T. Janicke, C.C. Landry, S.C. Christiansen, D. Kumar, G.D. Stucky, B.F. Chmelka, Aluminum incorporation and interfacial structures in MCM-41 mesoporous molecular sieves, J. Am. Chem. Soc. 120 (1998) 6940–6951.
[15] D.H. Brouwer, P.E. Kristiansen, C.A. Fyfe, M.H. Levitt, Symmetry-based ^{29}Si dipolar recoupling magic angle spinning nmr spectroscopy: a new method for investigating three-dimensional structures of zeolite frameworks, J. Am. Chem. Soc. 127 (2005) 542–543.
[16] C.A. Fyfe, H. Grondey, Y. Feng, G.T. Kokotailo, Natural-abundance two-dimensional silicon-29 MAS NMR investigation of the three-dimensional bonding connectivities in the zeolite catalyst ZSM-5, J. Am. Chem. Soc. 112 (1990) 8812–8820.
[17] N. Hedin, R. Graf, S.C. Christiansen, C. Gervais, R.C. Hayward, J. Eckert, B.F. Chmelka, Structure of a surfactant-templated silicate framework in the absence of 3D crystallinity, J. Am. Chem. Soc. 126 (2004) 9425–9432.
[18] S. Meiboom, D. Gill, Modified spin–echo method for measuring nuclear relaxation times, Rev. Sci. Instrm. 29 (1958) 688–691.
[19] E.D. Ostroff, J.S. Waugh, Multiple spin echoes and spin blocking in solids, Phys. Rev. Lett. 16 (1966) 1097–1098.
[20] A.N. Garroway, Homogeneous and inhomogeneous nuclear spin echoes in organic solids: adamantane, J. Magn. Reson. 28 (1977) 365–371.
[21] A.A. Maudsley, Modified Carr–Purcell–Meiboom–Gill sequence for NMR Fourier imaging applications, J. Magn. Reson. 69 (1986) 488–491.
[22] J. Perlo, F. Casanova, B. Blumich, 3D imaging with a single-sided sensor: an open tomograph, J. Magn. Reson. 166 (2004) 228–235.
[23] S. Ahola, J. Perlo, F. Casanova, S. Stapf, B. Bluemich, Multiecho sequence for velocity imaging in inhomogeneous RF fields, J. Magn. Reson. 182 (2006) 143–151.
[24] L. Pavesi, M. Balzarini, NMR study of the diffusion processes in gels, Magn. Reson. Imaging 14 (1996) 985–987.
[25] L.J. Zielinski, M.D. Huerlimann, Probing short length scales with restricted diffusion in a static gradient using the CPMG sequence, J. Magn. Reson. 172 (2005) 161–167.
[26] D.G. Rata, F. Casanova, J. Perlo, D.E. Demco, B. Bluemich, Self-diffusion measurements by a mobile single-sided NMR sensor with improved magnetic field gradient, J. Magn. Reson. 180 (2006) 229–235.
[27] M.L. Magnuson, B.M. Fung, Solvent suppression in proton NMR by the use of oxygen-17-enriched water, J. Magn. Reson. 99 (1992) 301–307.
[28] R.G. Bryant, T.M. Eads, Solvent peak suppression in high resolution NMR, J. Magn. Reson. 64 (1985) 312–315.

[29] B. Luy, J.P. Marino, ^{1}H-presup31P CPMG-correlated experiments for the assignment of nucleic acids, J. Am. Chem. Soc. 123 (2001) 11306–11307.

[30] H. Koskela, I. Kilpelainen, S. Heikkinen, L.R. Cahsqc, An application of a Carr–Purcell–Meiboom–Gill-type sequence to heteronuclear multiple bond correlation spectroscopy, J. Magn. Reson. 164 (2003) 228–232.

[31] K.E. Koever, G. Batta, K. Feher, Accurate measurement of long-range heteronuclear coupling constants from undistorted multiplets of an enhanced CPMG-HSQMBC experiment, J. Magn. Reson. 181 (2006) 89–97.

[32] J. Frahm, Multiple-pulse FT-NMR experiments for kinetic applications, J. Magn. Reson. 47 (1982) 209–226.

[33] P.F. Molitor, R.K. Shoemaker, T.M. Apple, Detection and structural characterization of rhodium dicarbonyls adsorbed in Y zeolites, J. Phys. Chem. 93 (1989) 2891–2893.

[34] A. Nordon, E. Hughes, R.K. Harris, L. Yeo, K.D.M. Harris, Direct measurement of the distance between adjacent guest molecules in a disordered solid inclusion compound using solid-state ^{19}F–^{1}H NMR spectroscopy, Chem. Phys. Lett. 289 (1998) 25–29.

[35] J.R. Harbridge, S.S. Eaton, G.R. Eaton, Comparison of electron spin relaxation times measured by Carr–Purcell–Meiboom–Gill and two-pulse spin–echo sequences, J. Magn. Reson. 164 (2003) 44–53.

[36] W.M. Witzel, S. Das Sarma, Multiple-pulse coherence enhancement of solid state spin qubits, Phys. Rev. Lett. 98 (2007) 077601-1–077601-4.

[37] J.T. Cheng, P.D. Ellis, Adsorption of Rb^{+} to γ-alumina as followed by solid-state ^{87}Rb NMR spectroscopy, J. Phys. Chem. 93 (1989) 2549–2555.

[38] D.L. Bryce, M. Gee, R.E. Wasylishen, High-field chlorine NMR spectroscopy of solid organic hydrochloride salts: a sensitive probe of hydrogen bonding environment, J. Phys. Chem. A 105 (2001) 10413–10421.

[39] A.S. Lipton, J.A. Sears, P.D. Ellis, A general strategy for the NMR observation of half-integer quadrupolar nuclei in dilute environments, J. Magn. Reson. 151 (2001) 48–59.

[40] R.W. Schurko, I. Hung, C.M. Widdifield, Signal enhancement in NMR spectra of half-integer quadrupolar nuclei via DFS-QCPMG and RAPT-QCPMG pulse sequences, Chem. Phys. Lett. 379 (2003) 1–10.

[41] I. Hung, A.J. Rossini, R.W. Schurko, Application of the Carr–Purcell–Meiboom–Gill pulse sequence for the acquisition of solid-state NMR spectra of spin-1/2 nuclei, J. Phys. Chem. A 108 (2004) 7112–7120.

[42] R. Siegel, T.T. Nakashima, R.E. Wasylishen, Application of multiple-pulse experiments to characterize broad NMR chemical-shift powder patterns from spin-1/2 nuclei in the solid state, J. Phys. Chem. B 108 (2004) 2218–2226.

[43] F.H. Larsen, H.J. Jakobsen, P.D. Ellis, N.C. Nielsen, High-field QCPMG-MAS NMR of half-integer quadrupolar nuclei with large quadrupole couplings, Mol. Phys. 95 (1998) 1185–1195.

[44] T. Vosegaard, F.H. Larsen, H.J. Jakobsen, P.D. Ellis, N.C. Nielsen, Sensitivity-enhanced multiple-quantum MAS NMR of half-integer quadrupolar nuclei, J. Am. Chem. Soc. 119 (1997) 9055–9056.

[45] R. Lefort, J.W. Wiench, M. Pruski, J.P. Amoureux, Optimization of data acquisition and processing in Carr–Purcell–Meiboom–Gill multiple quantum magic angle spinning nuclear magnetic resonance, J. Chem. Phys. 116 (2002) 2493–2501.

[46] J.Z. Hu, R.A. Wind, Sensitivity-enhanced phase-corrected ultra-slow magic angle turning using multiple-echo data acquisition, J. Magn. Reson. 163 (2003) 149–162.

[47] F.H. Larsen, I. Farnan, ^{29}Si and ^{17}O (Q)CPMG-MAS solid-state NMR experiments as an optimum approach for half-integer nuclei having long T_1 relaxation times, Chem. Phys. Lett. 357 (2002) 403–408.

[48] S.S. Hou, F.L. Beyer, K. Schmidt-Rohr, High-sensitivity multinuclear NMR spectroscopy of a smectite clay and of clay-intercalated polymer, Solid State Nucl. Magn. Reson. 22 (2002) 110–127.

[49] J. Trebosc, J.W. Wiench, S. Huh, V.S.Y. Lin, M. Pruski, Studies of organically functionalized mesoporous silicas using heteronuclear solid-state correlation NMR spectroscopy under fast magic angle spinning, J. Am. Chem. Soc. 127 (2005) 7587–7593.

[50] J.W. Wiench, Y.S. Avadhut, N. Maity, S. Bhaduri, G.K. Lahiri, M. Pruski, S. Ganapathy, Characterization of covalent linkages in organically functionalized MCM-41 mesoporous materials by solid-state NMR and theoretical calculations, J. Phys. Chem. B 111 (2007) 3877–3885.

[51] A. Bax, R. Freeman, S.P. Kempsell, Natural abundance carbon-13–carbon-13 coupling observed via double-quantum coherence, J. Am. Chem. Soc. 102 (1980) 4849–4851.

[52] C.A. Fyfe, Y. Feng, H. Gies, H. Grondey, G.T. Kokotailo, Natural-abundance two-dimensional solid-state ^{29}Si NMR investigations of three-dimensional lattice connectivities in zeolite structures, J. Am. Chem. Soc. 112 (1990) 3264–3270.

[53] A. Lesage, M. Bardet, L. Emsley, Through-bond carbon–carbon connectivities in disordered solids by NMR, J. Am. Chem. Soc. 121 (1999) 10987–10993.

[54] S. Huh, J.W. Wiench, J.-C. Yoo, M. Pruski, V.S.Y. Lin, Organic functionalization and morphology control of mesoporous silicas via a co-condensation synthesis method, Chem. Mater. 15 (2003) 4247–4256.

[55] F.H. Larsen, J. Skibsted, H.J. Jakobsen, N.C. Nielsen, Solid-state QCPMG NMR of low-γ quadrupolar metal nuclei in natural abundance, J. Am. Chem. Soc. 122 (2000) 7080–7086.

[56] Silicon sites can be described by a general formula $(\equiv SiO)_nSiR_m(OH)_{4-n-m}$. Sites with $m = 0$ are referred to as Q^n ($n = 0$–4); the functionalized materials may contain silicon atoms in positions denoted as T^n ($m = 1$ and $n = 0$–3) and D^n ($m = 2$ and $n = 0$–2).

[57] A.E. Dementyev, D. Li, K. MacLean, S.E. Barrett, Anomalies in the NMR of silicon: unexpected spin echoes in a dilute dipolar solid, Phys. Rev. B 68 (2003) 153302-1–153302-4.

[58] T.D. Ladd, D. Maryenko, Y. Yamamoto, E. Abe, K.M. Itoh, Coherence time of decoupled nuclear spins in silicon, Phys. Rev. B 71 (2005) 014401-1–014401-12.

[59] M.B. Franzoni, P.R. Levstein, Manifestations of the absence of spin diffusion in multipulse NMR experiments on diluted dipolar solids, Phys. Rev. B 72 (2005) 235410-1–235410-5.

[60] R.D. Black, M.B. Weissman, P.J. Restle, 1/f Noise in silicon wafers, J. Appl. Phys. 53 (1982) 6280–6284.

[61] B.M. Fung, A.K. Khitrin, K. Ermolaev, An improved broadband decoupling sequence for liquid crystals and solids, J. Magn. Reson. 142 (2000) 97–101.

[62] U. Haeberlen, J.S. Waugh, Coherent averaging effects in magnetic resonance, Phys. Rev. 175 (1968) 453–467.

[63] M. Ernst, A. Samoson, B.H. Meier, Low-power decoupling in fast magic-angle spinning NMR, Chem. Phys. Lett. 348 (2001) 293–302.

[64] G. De Paëpe, N. Giraud, A. Lesage, P. Hodgkinson, A. Boeckmann, L. Emsley, Transverse dephasing optimized solid-state NMR spectroscopy, J. Am. Chem. Soc. 125 (2003) 13938–13939.

[65] J.W. Wiench, C.E. Bronnimann, V.S.Y. Lin, M. Pruski, Chemical shift correlation nmr spectroscopy with indirect detection in fast rotating solids: studies of organically functionalized mesoporous silicas, J. Am. Chem. Soc. 129 (2007) 12076–12077.

[66] A.J. Vega, MAS NMR spin locking of half-integer quadrupolar nuclei, J. Magn. Reson. 96 (1992) 50–68.

[67] A.J. Vega, CP/MAS of quadrupolar $S = 3/2$ nuclei, Solid State Nucl. Magn. Reson. 1 (1992) 17–32.

[68] C.A. Fyfe, K.C. Wong-Moon, Y. Huang, H. Grondey, K.T. Mueller, Dipolar-based ^{27}Al–^{29}Si solid-state NMR connectivity experiments in zeolite molecular sieve frameworks, J. Phys. Chem. 99 (1995) 8707–8716.

[69] S.M. De Paul, M. Ernst, J.S. Shore, J.F. Stebbins, A. Pines, Cross-polarization from quadrupolar nuclei to silicon using low-radio-frequency amplitudes during magic-angle spinning, J. Phys. Chem. B 101 (1997) 3240–3249.

[70] M. Edén, J. Grins, Z. Shen, Z. Weng, Fast ^{29}Si magic-angle-spinning NMR acquisitions by RAPT-CP ^{27}Al ^{29}Si polarization transfer, J. Magn. Reson. 169 (2004) 279–283.

[71] Z. Yao, H.T. Kwak, D. Sakellariou, L. Emsley, P.J. Grandinetti, Sensitivity enhancement of the central transition NMR signal of quadrupolar nuclei under magic-angle spinning, Chem. Phys. Lett. 327 (2000) 85–90.

[72] J.W. Wiench, G. Tricot, L. Delevoye, J. Trebosc, J. Frye, L. Montagne, J.-P. Amoureux, M. Pruski, SPAM-MQ-HETCOR: an improved method for heteronuclear correlation spectroscopy between quadrupolar and spin-1/2 nuclei in solid-state NMR, Phys. Chem. Chem. Phys. 8 (2006) 144–150.

[73] J.P. Amoureux, M. Pruski, Theoretical and experimental assessment of single- and multiple-quantum cross-polarization in solid state NMR, Mol. Phys. 100 (2002) 1595–1613.

[74] C.P. Grey, A.J. Vega, Determination of the quadrupole coupling constant of the invisible aluminum spins in zeolite HY with ^{1}H/^{27}Al TRAPDOR NMR, J. Am. Chem. Soc. 117 (1995) 8232–8242.

[75] L. Delevoye, C. Fernandez, C.M. Morais, J.-P. Amoureux, V. Montouillout, J. Rocha, Double-resonance decoupling for resolution enhancement of ^{31}P solid-state MAS and ^{27}Al–^{31}P MQHETCOR NMR, Solid State Nucl. Magn. Reson. 22 (2002) 501–512.

[76] Y. Cai, R. Kumar, W. Huang, B.G. Trewyn, J.W. Wiench, M. Pruski, V.S.Y. Lin, Mesoporous aluminum silicate catalyst with single-type active sites: characterization by solid-state NMR and studies of reactivity for Claisen rearrangement reactions, J. Phys. Chem. C 111 (2007) 1480–1486.

[77] G.J. Kennedy, J.W. Wiench, M. Pruski, Determination of ^{29}Si–^{27}Al connectivities in zeolites with 2D ^{27}Al–^{29}Si RAPT-CPMG-HETCOR NMR. Solid State Nucl. Magn. Reson. (2008), doi:10.1016/j.ssnmr.2008.04.002.

[78] W. Sommer, J. Gottwald, D.E. Demco, H.W. Spiess, Dipolar heteronuclear multiple-quantum NMR spectroscopy in rotating solids, J. Magn. Reson. A 113 (1995) 131–134.

[79] Y.K. Lee, N.D. Kurur, M. Helmle, O.G. Johannessen, N.C. Nielsen, M.H. Levitt, Efficient dipolar recoupling in the NMR of rotating solids. A sevenfold symmetric radiofrequency pulse sequence, Chem. Phys. Lett. 242 (1995) 304–309.

[80] M. Haouas, F. Taulelle, Revisiting the identification of structural units in aqueous silicate solutions by two-dimensional Silicon-29 INADEQUATE, J. Phys. Chem. B 110 (2006) 3007–3014.

[81] S. Cadars, A. Lesage, N. Hedin, B.F. Chmelka, L. Emsley, Selective NMR measurements of homonuclear scalar couplings in isotopically enriched solids, J. Phys. Chem. B 110 (2006) 16982–16991.

[82] L. Duma, W.C. Lai, M. Carravetta, L. Emsley, S.P. Brown, M.H. Levitt, Principles of spin–echo modulation by J-couplings in magic-angle-spinning solid-state NMR, ChemPhysChem 5 (2004) 815–833.

[83] S. Cadars, A. Lesage, L. Emsley, Chemical shift correlations in disordered solids, J. Am. Chem. Soc. 127 (2005) 4466–4476.